RSC Advances

PAPER

View Article Online
View Journal | View Issue

Cite this: *RSC Adv.*, 2021, **11**, 31746

Efficacy and safety of scleral crosslinking using poly(ethylene glycol)ether tetrasuccinimidyl glutarate for form-deprivation myopia progression in rabbits

Yanbing Wang,[a] Zhenquan Wu,[a] Bingqian Liu,[a] Jiang Lu,[b] Silvia Tanumiharjo,[a] Jianbing Huang,[†b] Xiujuan Zhao[†a] and Lin Lu[†a]

Myopia is becoming increasingly prevalent worldwide at an alarming rate. However, no effective treatment is available for inhibiting myopia progression. Materials chemistry advancements have made it possible to regulate mechanical properties and rate of degradation with good compatibility by developing newly crosslinking systems such as the branched polyethylene glycol (PEG) systems. Herein, we presented a PEG molecule with *N*-hydroxysuccinimide (NHS) ester functional groups at the chain ends as a macromolecular crosslinking agent for the treatment of myopia. We found that the scleral collagen crosslinked with the four-armed star-shaped PEG molecule with NHS ester functional group (4S-PEG) showed better biomechanical properties, increased thermal stability and higher resistance to degradation. 4S-PEG exhibited relatively low cytotoxicity for human fetal scleral fibroblasts. The retrobulbar injection of 4S-PEG at a relatively low concentration (2.5 mM) showed good effective control of the progression of form-deprivation myopia in rabbits. There were no signs of adverse effect or damage by repeated injections with 4S-PEG in rabbits. The results of this work demonstrate that 4S-PEG can serve as a robust macromolecular crosslinking agent and is expected to have promise for application in the treatment of the progression of myopia.

Received 19th July 2021
Accepted 19th September 2021

DOI: 10.1039/d1ra05533j

rsc.li/rsc-advances

1. Introduction

Globally, myopia has become a major public health concern and is one of the leading socioeconomic burdens.[1,2] Myopia is a risk factor of cataracts, open-angle glaucoma, myopic retinal detachment and macular degeneration. The development of these conditions can result in irreversible visual impairment and is correlated to the growth in the axial length and degree of myopia.[3]

Scleral thinning, loss of scleral tissue and biomechanical scleral weakening are associated with myopia progression, especially in pathological myopia.[4,5] Scleral crosslinking, including physical and chemical crosslinking, is a rising new treatment that shows promise. Physical crosslinking (UVA–riboflavin crosslinking) has shown great success in treating biomechanically weakening corneas.[6] However, previous studies have shown that physical scleral crosslinking leads to photoreceptor loss.[7–9] In addition, it is challenging to apply radiation to the posterior sclera, to which scleral thinning in myopia progression is primarily restricted.[10–13]

Chemical crosslinking could be a more effective method in treating the posterior pole. To date, various crosslinking agents, mostly small molecules, have been developed to stiffen the sclera. Glutaraldehyde, glyceraldehyde[14,15] and genipin are often used as crosslinking agents reacting with protein amines. However, glutaraldehyde, as a strong sterilant and irritant, is toxic to cells and tissues. Glyceraldehyde, on the other hand, was not effective in slowing myopia progression in comparison to normal control eyes.[15] Furthermore, advanced glycation end products (AGEs) that are related to aging as well as diabetic complications, are produced during nonenzymatic glycosylation reaction with glyceraldehyde.[16,17] Collagen crosslinking induced by genipin has been demonstrated to improve biomechanical properties of the sclera in porcine[18] and rabbits.[19] This effect of treatment is dose-dependent. Form-deprivation myopia in guinea pig and tree shrews was effectively blocked by scleral crosslinking only at a high dose of genipin.[20,21] However, previous study reported that the toxicity of genipin is also dose-dependent and acute.[22] The relative genotoxicity and low 50% lethal dose values were observed in cell studies.[23,24] Wang *et al.*[22] suggested that the concentration of genipin should be controlled to within 0.5 mM in tissue engineering, which is much lower than the dose of treatment in

[a]*State Key Laboratory of Ophthalmology, Zhongshan Ophthalmic Center, Sun Yat-sen University, Guangzhou, 510060, China. E-mail: lulin@gzzoc.com*

[b]*Key Laboratory for Polymeric Composite and Functional Materials of Ministry of Education, Guangdong Provincial Key Laboratory for High Performance Resin-based Composites, School of Chemistry, Sun Yat-sen University, Guangzhou, 510275, China*

† These authors contributed equally.

myopia controlling. Therefore, the treatment of myopia imposes the need for development of new crosslinking approaches.

In recent years, macromolecular crosslinking agents have attracted considerable attention. Compared to small molecules, polymers possess several bio- or physicochemical advantages, such as high stability and biocompatibility, structural and functional diversity and tunable solubility.[25] The utilization of appropriate polymeric crosslinking agents can overcome the shortcomings of micromolecular agents, and such agents have shown promise for application in treating myopia.

In this regard, at the first time we report the use of *N*-hydroxysuccinimide (NHS) ester-terminated polyethylene glycol (PEG) as macromolecular crosslinking agents to evaluate the effect on the biological properties of the sclera after crosslinking. As shown in Fig. 1, NHS esters were introduced at the chain ends due to the high reaction efficiency of NHS esters with the primary amino group from the lysine residues on the native protein *via* the formation of stable amide bond.[26] Scleral collagen, mainly type I collagen, accounts for 50% of the total weight of scleral tissue.[27] Therefore, the NHS-terminated PEG star polymer can form stable amide bonds through a condensation reaction,[28] which contributes to the cross-linking of collagen fibers and enhances the biomaterial properties of collagen.[29–31] Moreover, the pegylation of NHS esters can provide several significant pharmacological advantages, such as improved reagent solubility, reduced dosage frequency, no reduction in efficacy with a potential reduction in toxicity, extended circulation, increased reagent stability, and enhanced protection from proteolytic degradation.[32,33]

The performance of this type of macromolecular crosslinking agents needs to be further confirmed *in vitro* and *in vivo*. Thus, we investigated herein this type of macromolecular crosslinking agents in different molecular weights and different structures (linear and star-shaped structures) *in vitro* and then select the optimal agent for retrobulbar injection to assess its efficacy and safety in myopia treatment *in vivo* in this study.

2. Materials and methods

2.1 Materials and reagents

Porcine eyes were acquired from a local slaughter house. Each 4.0 mm × 12.0 mm scleral strip was cut vertically at the 12 o'clock position beside the root of the optic nerve using a custom-made double-blade scalpel. The strips were covered with 0.2% hydroxypropyl emthylcellulose gel before the tests. The four-armed PEG with NHS esters groups at the chain ends (MW = 2000, 5000 and 10 000 Da) (4S-PEG) and linear PEG with NHS esters groups at the chain ends (MW = 10 000 Da) (SG-PEG-SG) were purchased from JenKem Technology (Texas, USA). The samples treated with phosphate-buffered saline (PBS, Gibco, USA) and four-armed PEG raw material (4S-PEG–OH, MW = 10 000 Da) (JenKem Technology, USA) performed as control groups. The structures and the degrees of functionalization of all PEG materials were confirmed from MALDI and ^{1}H-NMR using dimethyl sulfoxide-d_6 (DMSO-d_6). All other materials and reagents were stated in the corresponding place.

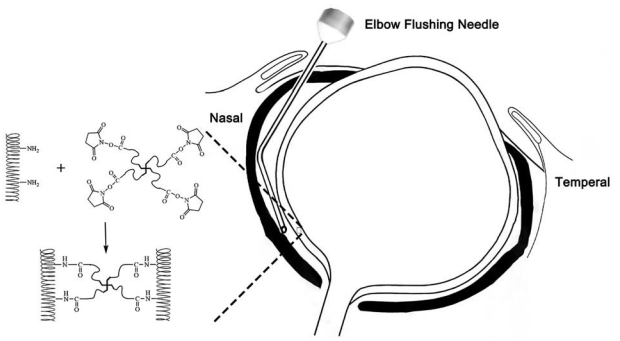

Fig. 1 Reaction between type I collagen and poly(ethylene glycol) ether tetrasuccinimidyl glutarate (4S-PEG).

2.2 Cell study

All procedures were performed in a cell culture room using sterile instruments and vessels. Human fetal scleral fibroblasts (HFSFs) were obtained from college of life sciences at Wuhan University and conserved in Dulbecco's modified Eagle's medium (Gibco, USA) with 1% antibiotic/antimycotic (penicillin–streptomycin, GE HyClone, USA) and 10% (v/v) fetal bovine serum (Zeta Life, Australia Origin) at 37 °C in 5% CO_2. All the cells were trypsinized upon reaching 90% confluence, then seeded in 96-well (1×10^4 cells per well) plates for subsequent experiments. After attaching to the substrate, HFSFs were incubated in 96-well plates (1×10^4 cells per well) with culture medium containing PBS/PEG derivatives for 24 h. Preliminary experiments were done to determine the approximate concentration range of PEG derivatives. The number of cells exposed to various concentrations of PBS/PEG derivatives was quantified by Cell Counting Kit-8 (CCK-8) assay (Dojindo Laboratories, Kumamoto, Japan).

2.3 Scleral collagen crosslinking

Each strip was washed by 1× PBS three times. The PBS remaining on the scleral surface was absorbed with filter paper. The scleral strips were immersed in PBS, 4S-PEG–OH, SG-PEG-SG and 4S-PEG with different molecular weight (MW = 2000, 5000 and 10 000 Da) in different concentrations in PBS (0.5 mM, 1 mM, 2.5 mM) for 24 h at 37 °C.

2.4 Uniaxial mechanical testing

The porcine scleral strips (4 mm × 12 mm) after crosslinking with PBS/PEG derivatives were submerged in 0.2% hypromellose eye gel. The scleral thickness was measured using a digital laser displacement sensor (MTI, USA) before stress–strain tests were performed. The scleral strips were clamped vertically with a 4 mm interval between the fixtures of an Instron 3343 microtester (Instron, USA). Five pre-loading cycles with an upper limit of 0.01 N were applied to each strip. The strip was loaded to destruction at 2 mm min^{-1} after pre-loading. The elastic modulus at 8%, 10%, 12% and 20% strain was compared among different groups.

2.5 Thermal stability

The denaturation temperature was determined using a differential scanning calorimetry (DSC) instrument (TA Q20, USA). The excess solution from samples after crosslinking was absorbed with filter paper. Samples were cut into 4 mm × 4 mm pieces and put into a standard aluminum pans. The pans were fastly sealed using a DSC pan sealing press and transferred to the test table. An empty aluminum pan was used as reference probe. Heating was carried out at a constant temperature ramp of 5 °C min^{-1} in the temperature range of 40–80 °C, and the apparent thermal denaturation peak was recorded in denaturation curves.

2.6 Collagenase degradation

Collagenase type I purchased from MP Biomedicals (California, USA) was dissolved in 1× PBS (pH 7.4) to form 25 IU ml^{-1} collagenase solution. Each scleral sample (4 mm × 12 mm) was cut into 4 mm × 4 mm pieces. The adjacent two scleral pieces were randomly assigned to two groups, which were treated with PBS or crosslinking agent respectively. The samples after crosslinking by PBS/PEG derivatives were dried with filter paper and weighed as the initial weight. The scleral pieces were incubated in the prepared solution with collagenase type I. The adjacent two scleral pieces are compared by themselves in weight to assess the degree of the resistance to enzyme degradation. At fixed time points, the samples were repeated the above operation and recorded the weights. The weight difference between two scleral pieces in each group was plotted as a function of time.

2.7 Animals study

Sixteen three week-old white New Zealand rabbits that weighed 260–550 g were subjects of this study. All animals were obtained from the Xin Hua Animal Breeding Unit in Guangzhou and randomly assigned to one of the following two groups, with eight animals per group: the 4S-PEG group (form-deprivation myopia eyes treated with 4S-PEG) and the PBS group (form-deprivation myopia eyes treated with PBS). The contralateral (left) eye was free of form deprivation and served as the normal control. All procedures were carried out in accordance with the ARVO Statement on the Use of Animals in Ophthalmic and Visual Research. This experimental protocol was approved by the Institutional Animal Care and Use Committee of Sun Yat-sen University (2020-035).

2.7.1 Form deprivation procedure. Form deprivation was achieved by firmly gluing a hand-made translucent latex occluder to the fur forwards on the right forehead and hanging on the ear backward, which was easy to wear and remove. The left forehead, nose, and mouth remained exposed. No stretch, compression or restriction was ensured on the movement of the eyelid and enough space was able for the occluded eye to blink freely. The translucent occluder was examined twice daily to ensure that it was in place and continued to fit well.

2.7.2 Crosslinking procedure. General anesthesia for all animals was performed with 1 mg kg^{-1} xylazine hydrochloride (25 mg ml^{-1}, intramuscular injection) and 10 mg ml^{-1} pentobarbital sodium (20 mg kg^{-1}, intravenous injection). In addition, 0.5% tetracaine hydrochloride was instilled for local anesthesia. Gentle pressure was applied toward the lower eye rim such that the eye slightly bulged from the orbit. Then, an approximately 1 mm conjunctival incision was made in the nasal quadrant of the right eye (3 o'clock position) with a pair of scissors. The elbow flushing needle was kept parallel to the wall of the orbit through the conjunctival incision and angled down at the equator of the eyeball. A retrobulbar injection of 0.2 ml of 2.5 mM 4S-PEG or PBS was administered in the nasal quadrant using a flat needle (Fig. 1). The eye slightly bulged outward during the injection. The injections were given nine times at a time interval of one week between injections. After each injection, Tobradex eye ointment (Alcon, USA) was applied.

2.7.3 Biometric measurements. An iCare TONOVET rebound tonometer (iCare Finland), which averages five successful readings, was used to measure the intraocular pressure (IOP) of each eye. Topical 1% tropicamide was used to induce cycloplegia, and then direct ophthalmoscopy was performed to exclude eye diseases before the experiment and the possibility of damage after the retrobulbar injections. An ARK-30 Autorefractor/Keratometer (Nidek, Japan) was used to measure corneal curvature and refractive error one day before injection. These measurements were obtained three times in each eye. The reported corneal curvatures are the mean of horizontal as well as vertical meridian *K*-values. The refractive diopter recorded was the mean of the three spherical equivalents. A Cinescan S system (Quantel Medical, France) measured the anterior chamber depth, lens thickness, vitreous chamber depth and axial length after refractive error measurements were obtained. Data from at least five separate probe locations were recorded and averaged for the measurement of axial ocular dimensions.

Full-thickness retinal and choroidal structures were observed using optical coherence tomography (OCT, Heidelberg, Germany) in the beginning of the experiment and once a month before sacrificing. All layers in the posterior pole and around the optic disk are the object of our regular observation using OCT.

2.7.4 Biomechanical measurements. After eight weeks, the animals were sacrificed with an overdose injection of xylazine hydrochloride and pentobarbital sodium. After sacrifice, the procedure to obtain the scleral strip (4 mm × 12 mm) was the same as that in porcine. After the scleral thickness was measured, the scleral strips were clamped vertically with a 4 mm interval between the fixtures of the microtester. After five times preload cycles, the elastic modulus was calculated between tensile loads of 0.04 N and 0.07 N, which was considered to be the physiological level.[34] The creep rate (percent extension per hour) was computed as the creep extension over the period from 300 to 1150 seconds after loading. The creep extension of all samples was recorded under one steadily load of 0.07 N for 20 minutes at room temperature. The creep extension divided by the interval between 300 and 1150 seconds after loading is considered as the creep rate.[35]

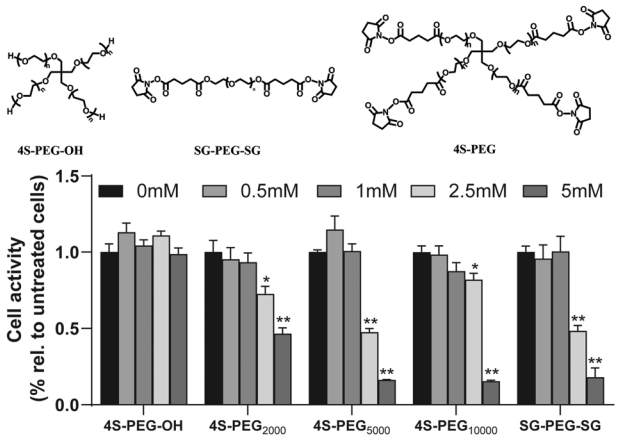

Fig. 2 Structure of the three PEG derivatives and assessment of HFSFs viability by CCK-8 assay. Viability of HFSFs incubated with various concentrations of 4S-PEG–OH, 4S-PEG_{2000}, 4S-PEG_{5000}, 4S-PEG_{10000} and SG-PEG-SG *in vitro*. * indicates $p < 0.05$, ** indicates $p < 0.01$.

2.7.5 Histology. The histological samples were immersed in tissue fixative (4% paraformaldehyde and 1% glutardialdehyde) for at least three days and then dehydrated with a graded alcohol series, passed through a series of xylene solutions, and infiltrated with wax. Each wax-embedded bulbus oculi was cut into 4 μm-thick sections sagittally along the plane between the cornea and the optic disc.

To observe the histological changes, 4 μm-thick wax-embedded sections were prepared for staining with hematoxylin and eosin (H&E). Apoptotic cells were detected using a TUNEL (TdT-mediated dUTP nick-end labeling) assay kit (Promega, USA) according to the manufacturer's instructions. A light microscope (Zeiss, Germany) evaluated the specimens at various magnifications. The number of TUNEL-positive cells was counted manually per field.

For examination by electron microscopy, the fixed tissue was washed in PBS, followed by two-hour postfixation with 1% osmium tetroxide, and dehydrated in a graded alcohol series and finally 100% acetone. The dehydrated samples were embedded in a graded epoxide resin (Sigma, Germany) and

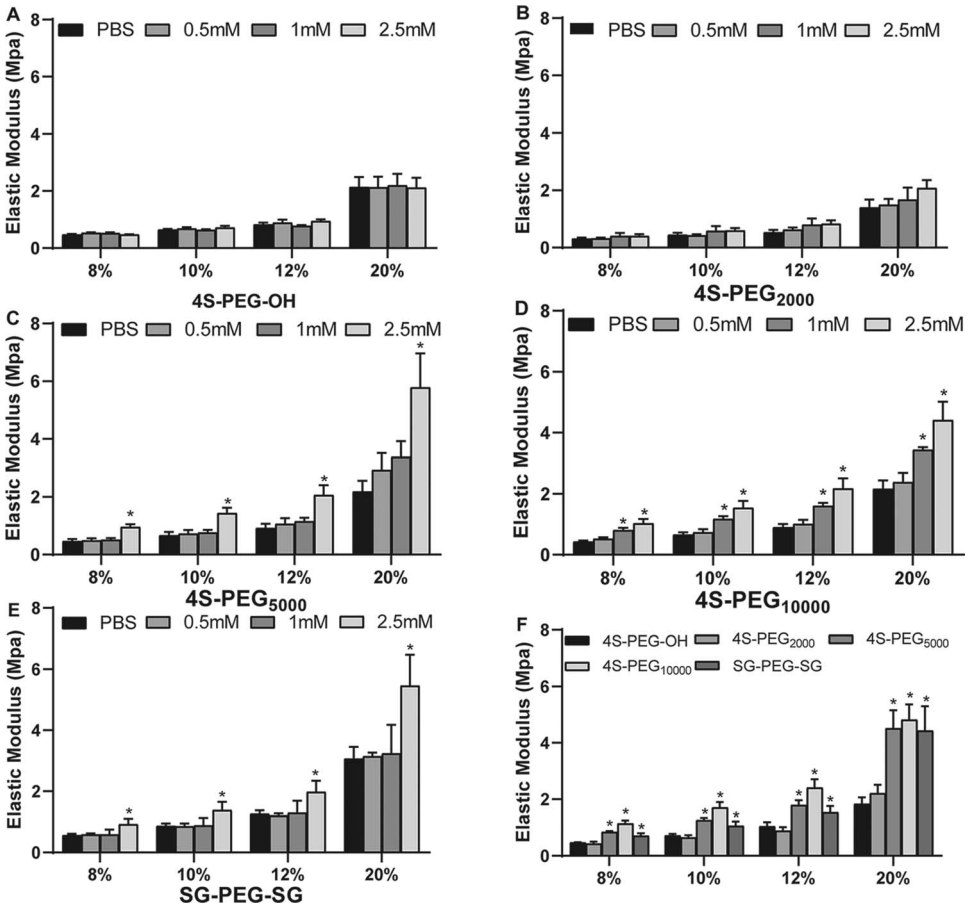

Fig. 3 Assessment of uniaxial mechanical testing. (A) and (B) The strips crosslinked with 4S-PEG–OH and 4S-PEG_{2000} at various concentrations had no significant effect on its modulus of elasticity ($p > 0.05$). (C)–(E) The strips crosslinked with 4S-PEG_{5000}, 4S-PEG_{10000} and SG-PEG-SG at various concentrations all showed significant dose dependence in elastic modulus. The strips crosslinked with 4S-PEG_{5000} and SG-PEG-SG showed significant difference at 2.5 mM from the noncrosslinked sclera strips ($p < 0.05$). The strips crosslinked with 4S-PEG_{10000} showed significant difference at 1 mM and 2.5 mM. (F) The strips crosslinked with 4S-PEG–OH, 4S-PEG_{2000}, 4S-PEG_{5000}, 4S-PEG_{10000} and SG-PEG-SG were compared at 2.5 mM. * indicates $p < 0.05$.

acetone mixture (1 : 3, 1 : 1, 3 : 1) each for one hour. They were then incubated in pure epoxide resin overnight. The embedded tissue was sectioned at a thickness of 100 nm by the ultramicrotome (Leica UC7, Germany). After stained with uranyl acetate and lead citrate, serial ultrathin sections were studied using a transmission electron microscope (Tecnai G2 Spirit, FEI, USA).

2.8 Statistical analysis

All statistical analyses were processed using SPSS version 23 software. Continuous values are presented as the mean ± standard error (SE). A *t*-test or M−W test was performed on comparisons between two groups or between the treated and untreated eyes. Multiple means were compared among the multiple groups by one-way analysis of variance (ANOVA) or K–W test. A *P* level less than 0.05 was considered statistically significant.

3. Result and discussion

3.1 Cell study

The cytotoxicity of the three PEG derivatives with different structures (Fig. 2) was evaluated *via* the CCK-8 assay. The results of the CCK-8 assay demonstrated that HFSFs incubated with 4S-PEG–OH remained viable even at a concentration of 5 mM and all other PEG derivatives exhibited toxicity to HFSFs in a dose-dependent manner (Fig. 2). The activity of HFSFs treated with PEG derivatives at doses above 2.5 mM showed statistically difference from the control group. However, HFSFs incubated 4S-PEG_{10000} at a concentration of 2.5 mM remained mostly viable (>80% of the control).

3.2 Evaluation of crosslinking efficacy

Scleral samples were then crosslinked with four commercially available crosslinking agents 4S-PEG_{2000}, 4S-PEG_{5000}, 4S-PEG_{10000} and SG-PEG-SG compared with 4S-PEG–OH as the control group. Notably, there were no significant differences in the degree of NHS end-group functionalization of the PEG derivatives (4S-PEG_{2000} 94.7%, 4S-PEG_{5000} 95.3%, 4S-PEG_{10000} 96.0% and SG-PEG-SG 97.6%, quantified by ^{1}HNMR and MALDI-TOF). Since biophysical properties are of most concern for scleral crosslinking, mechanical testing of the porcine scleral strips crosslinked with 4S-PEG–OH, 4S-PEG_{2000}, 4S-PEG_{5000}, 4S-PEG_{10000} and SG-PEG-SG was carried out. Fig. 3 showed the elastic modulus gradients of the porcine sclera strips after cross-linking. The strips crosslinked with 4S-PEG–OH and 4S-PEG_{2000} at various concentrations had no significant effect on its modulus of elasticity (Fig. 3A and B). However, differences were observed for modulus of elasticity at non-crosslinked sclera strips from the rest three crosslinked strips. The strips with different crosslinking concentrations showed significant dose dependence in elastic modulus (Fig. 3C–E). There were significant differences between the noncrosslinked groups and 4S-PEG_{10000} at 1 mM and 2.5 mM. And the elastic modulus of strips crosslinked with 2.5 mM 4S-PEG_{10000} at 8%, 10% and 12% was the highest increase relative to those crosslinked with other agents (Fig. 3F).

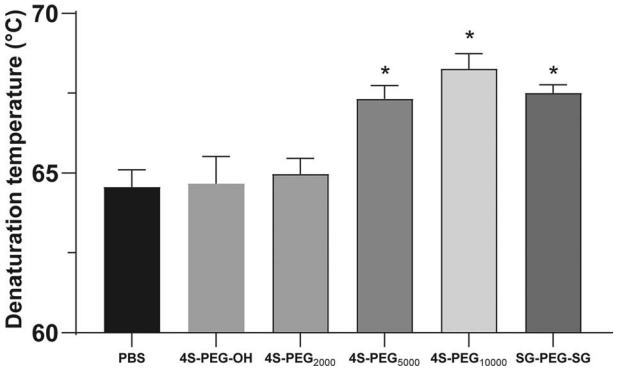

Fig. 4 Denaturation temperature of scleral collagen evaluated in this study. Values are presented as mean ± SE (n = 3). Noncrosslinked sclera exhibited a denaturation temperature of 64.57 ± 0.76 °C. 4S-PEG–OH and 4S-PEG_{2000} showed no significantly difference (p > 0.05). The strips crosslinked with 4S-PEG_{5000}, 4S-PEG_{10000} and SG-PEG-SG showed significant difference compared with noncrosslinked sclera. 4S-PEG_{10000} crosslinked sclera exhibited the highest denaturation temperatures. * indicates p < 0.05.

The thermal properties of scleral collagen treated by different crosslinking agents at the concentration of 2.5 mM were evaluated by DSC. Fig. 4 showed the denaturation temperatures of all samples. Noncrosslinked sclera exhibited a denaturation temperature of 64.57 ± 0.76 °C. The 4S-PEG_{10000} exhibited the highest denaturation temperatures (68.27 ± 0.66 °C, p < 0.05).

Moreover, collagenase degradation experiments also demonstrate that 4S-PEG_{10000} has the highest resistance to enzymatic degradation (Fig. 5). According to the experimental results of collagenase degradation, we considered the use of weekly retrobulbar injections for *in vivo* myopia treatment.

Based on *in vitro* experiments, it was found that compared to other PEG derivatives with different molecular weight of stellate structure and linear structure, 4S-PEG with molecular weight 10 000, especially at a concentration of 2.5 mM, crosslinked with scleral collagen, could significantly enhance its biomechanical properties, its thermal stability and resistance to

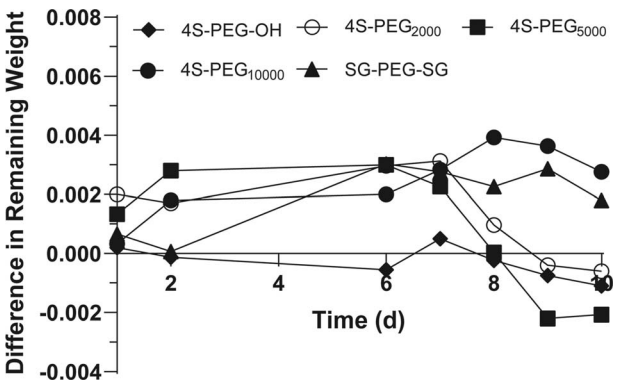

Fig. 5 Collagenase degradation of 4S-PEG–OH, 4S-PEG_{2000}, 4S-PEG_{5000}, 4S-PEG_{10000} and SG-PEG-SG up to 9 days *in vitro*. 4S-PEG_{10000} showed the highest resistance to enzymatic degradation compared with other three strips (ANOVA, p < 0.05, n = 3).

enzymatic degradation in a relatively safe range. Although 4S-PEG with a lower molecular weight should have a higher crosslinking density, the crosslinker with longer PEG arms also leads to increased hydrogen bonding around the proteins in sclera and thus the higher biomechanical properties, thermal stability and resistance to enzymatic degradation.[36] Therefore, we chose 2.5 mM 4S-PEG (MW = 10 000) to further investigate the efficacy and safety of scleral crosslinking in myopia controlling in animal experiments.

3.3 Animal study

3.3.1 Changes in ocular components. The myopia induced in 3 week-old New Zealand rabbits by covering the eyelid with a translucent occluder for 56 days was probably attributable to visual regulation, in which there was no feedback to limit growth, and the eye continued to grow until natural bodily reductions occurred. Comparing the interocular difference between the form-deprived eye (right eye, OD) and the uninduced eye (left eye, OS), we intend to further validate the efficacy of the treatment group (4S-PEG group) relative to the control group (PBS group). Changes in refractive error and ocular components, especially the vitreous chamber depth and axial length, are the main features of myopia progression, and were thus understandably the focus of our research.

Fig. 6A shows changes in the mean interocular difference (OD–OS) in refractive error in the PBS and 4S-PEG groups. The mean interocular difference in refractive error was 0.29 ± 0.14 D in the PBS group and 0.46 ± 0.79 D in the 4S-PEG group before form deprivation. There were no significant differences in the mean interocular difference in refractive error in two groups at the start of the study. A significant treatment effect on slowing form-deprived myopia was observed in the 4S-PEG group after 28 days ($P < 0.05$). After 56 days of form deprivation, the mean interocular difference in refractive error was −2.17 ± 0.84 D in the PBS group, and 0.46 ± 0.62 D in the 4S-PEG group.

The mean interocular difference (OD–OS) in axial length in the two groups was plotted as a fitting curve function of the

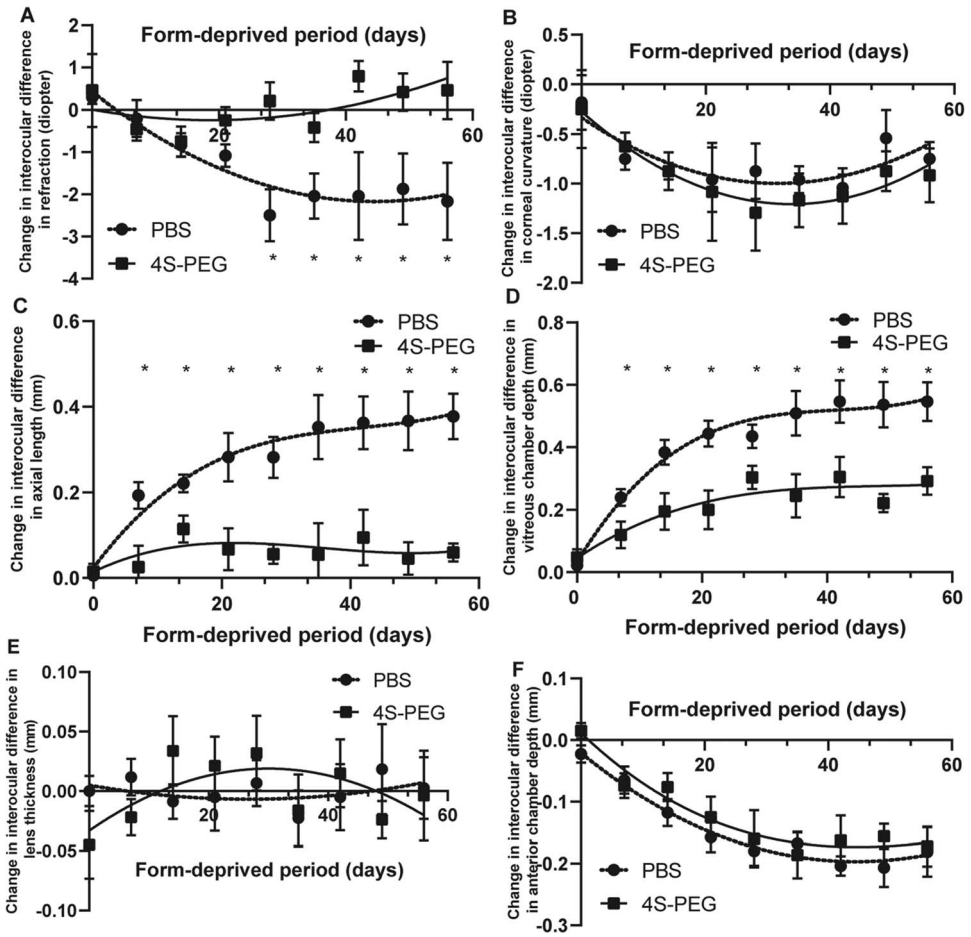

Fig. 6 Developmental changes in the mean interocular difference (OD–OS) in each group in rabbits (measured at 0, 7, 14, 21, 28, 35, 42, 49 and 56 days) plotted as a fitting curve function of the form-deprivation period. (A) The mean interocular difference in refractive error was significantly smaller in the PBS group than in the 4S-PEG groups from days 28 to 56 (*). (B) The mean interocular difference in corneal curvature decreased in a similar manner in the two groups after 56 days of form deprivation. There was no difference between the groups at the start or end of the study. The axial length changes (C) and the vitreous chamber depth changes (D) were consistent, which were smaller in the 4S-PEG group than in the PBS group from days 7 to 56 (*). Developmental changes in the lens thickness (E) and anterior chamber depth (F) in both groups were identical, with no significant differences in the two groups. The anterior chamber depth of the right eye in two groups increased much slower than that of the left eye. There were no intergroup differences at any time point. A significant difference is indicated by * for $P < 0.05$.

form-deprived period (Fig. 6C). The relative ocular elongation between the two eyes in two groups was significantly different after 7 days of form deprivation ($P < 0.05$). After 56 days of form deprivation, the interocular difference in axial length was smaller in the 4S-PEG group (0.06 ± 0.02 mm) than in the PBS group (0.38 ± 0.05 mm).

The developmental changes in the vitreous chamber depth were consistent with those in the axial length. The mean interocular difference (OD–OS) in vitreous chamber depth in the two groups was plotted as a fitting curve function of the form-deprivation period (Fig. 6D), which revealed a significant increase in the right eye in the PBS group compared to that in the 4S-PEG group ($P < 0.05$) from 7 days of occlusion. At the end of the study, the interocular difference in vitreous chamber depth was 0.55 ± 0.06 mm in the PBS group, and 0.29 ± 0.04 mm in the 4S-PEG group.

The fitting curve functions of the interocular difference (OD–OS) in other ocular component (corneal curvature, anterior chamber depth and lens thickness) in two groups were almost coincident (Fig. 6B, E and F). There were no intergroup differences at any time point ($P > 0.05$, all).

Deprivation-induced ocular elongation arose from significant increases in the vitreous chamber depth in form-deprived eyes. At the end of the occlusion phase (56 days), the form-deprived eyes treated with 4S-PEG showed a significantly smaller increase in the vitreous chamber depth and axial length and significantly smaller refractive error changes than those treated with PBS.

3.3.2 Changes in biomechanical properties of the sclera. Moreover, we investigated the biomechanical properties of the sclera in rabbits after sacrifice. The posterior sclera in the form-deprived eye of rabbits treated with PBS or 4S-PEG (0.25 ± 0.01 mm and 0.25 ± 0.01 mm, respectively) was significantly thinner ($P < 0.05$) than that in the contralateral control eye (0.28 ± 0.01 mm and 0.28 ± 0.02 mm). This reduced thickness, as an important feature of progressive myopia, is consistent with the results of other studies.[37–41] There was no significant intraocular difference in the mean thickness of the posterior sclera among the scleral samples from the two groups.

Biomechanical properties of the sclera, including the elastic modulus and creep rate, were evaluated. Compared with the posterior sclera in the untreated left eye (2.32 ± 0.06 MPa), the elastic modulus in the treated right eye in the 4S-PEG group (3.30 ± 0.12 MPa) was increased ($P < 0.05$), while that in the treated right eye in the PBS (1.87 ± 0.13 MPa) was decreased ($P < 0.05$) (Fig. 7A). Fig. 7C showed a significant increase in the creep rate in samples from the right eye in the PBS group (3.38 ± 0.28% per h) compared with that in samples from the left eye

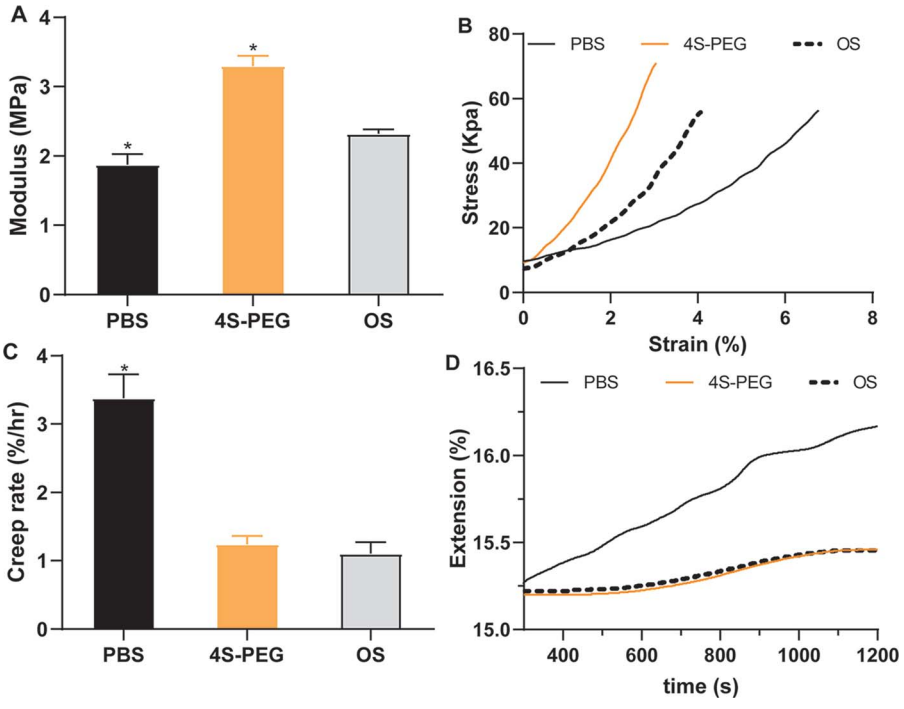

Fig. 7 Comparison of the elastic modulus and creep rate at 0.07 N of sclera between the operated and unoperated eyes. (A) The elastic modulus of posterior scleral samples from the eyes treated with PBS or 4S-PEG and left control eye (OS) was recorded. The elastic modulus was decreased in samples from the eyes treated with PBS (*) and increased in samples from the eyes treated with 4S-PEG compared with samples from the left eye. (B) The typical examples of the stress-*versus*-strain curves of posterior scleral strips from the treated and untreated eyes of rabbits were shown. (C) The creep rate at 0.07 N of posterior scleral samples from the right eye and left eye in the two groups was recorded. There was a significant increase in the creep rate of samples from the right eye in the PBS group (*) compared with that of samples from the left eye. The creep rate in samples from the right eye in the 4S-PEG group was not significantly different from that in samples from the left eye. (D) The typical examples of the extension-*versus*-time curves of posterior scleral strips from the treated and untreated eyes of rabbits were shown. A significant difference is indicated by * for $P < 0.05$.

(1.10 ± 0.16% per h). The creep rate in samples from the right eye in the 4S-PEG group (1.24 ± 0.10% per h) was not significantly different from that in samples from the left eye.

In the present study, posterior scleral samples from form-deprived eyes treated with 4S-PEG showed a significant increase in elastic modulus and a significant decrease in creep rate compared with PBS-treated eyes, which reaffirmed the

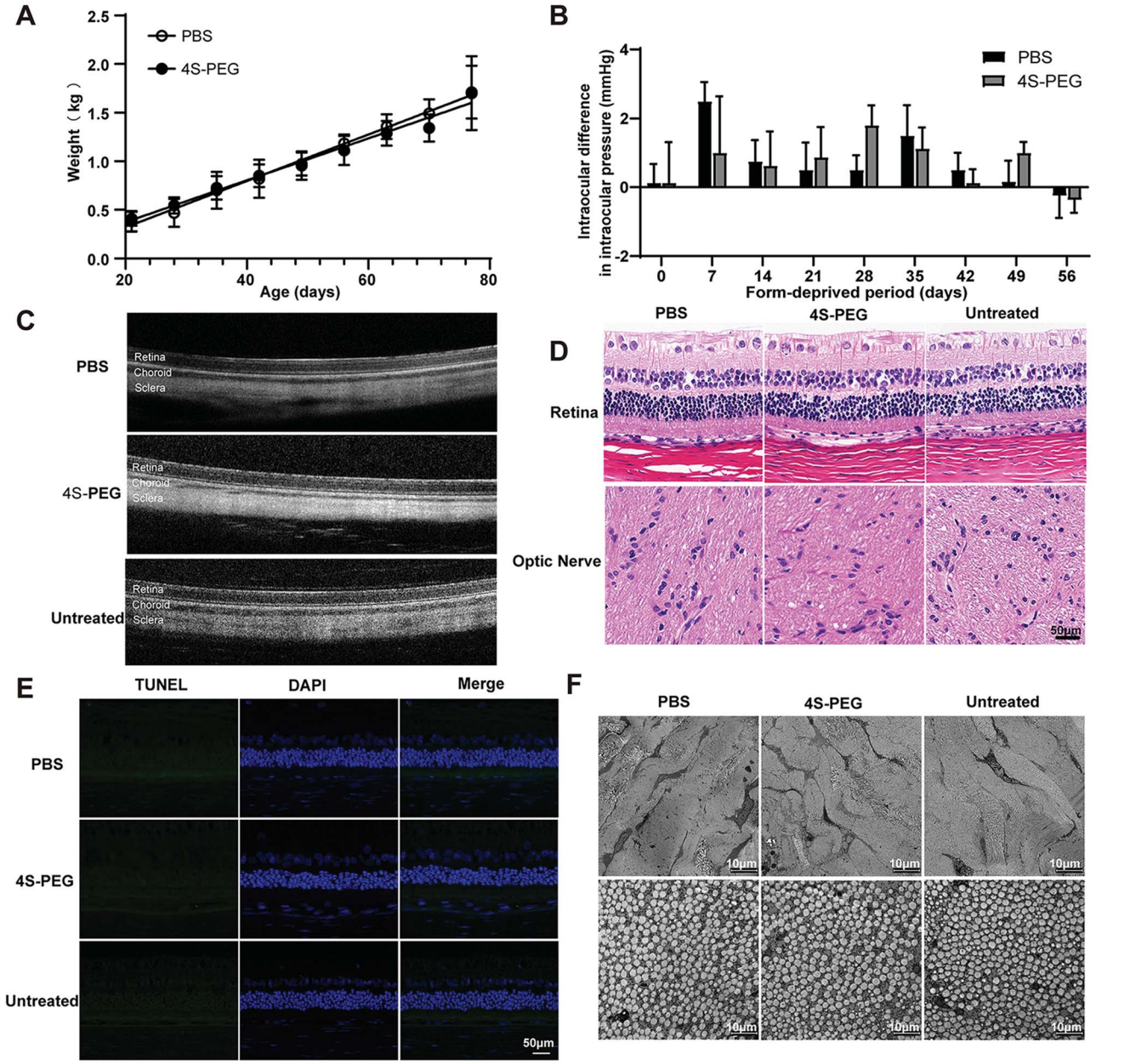

Fig. 8 (A) Developmental changes in weight plotted as a fitting curve function of age for rabbits in the two groups. (B) The mean changes in the interocular difference in IOP from baseline were small, and the intergroup differences were not statistically significant through 56 days after the first retrobulbar injection of PBS or 4S-PEG. Nevertheless, there was an increasing trend at the beginning of the injection regimen. On day 56, there were no significant differences between the two eyes. (C) Retinal and choroidal structures observed by OCT in the right eye of representative rabbits from the PBS group and the 4S-PEG group compared with the unoperated left eye. Various safety assessments were performed to examine the untreated and treated eyes (treated with PBS or 4S-PEG), including H&E staining and TUNEL staining of paraffin-embedded sections of the globe (200×) and transmission electron microscopy of semithin scleral sections (960× and 6800×). (D) The retina, choroid, sclera and optic nerve in H&E-stained sections of all eyes showed typical features. (E) Apoptotic cells were determined by TUNEL assay and DAPI staining (blue). TUNEL-positive apoptotic cells were detected by localized FITC fluorescence (green). There were no fluorescent TUNEL-positive (green) cells in the sclera, choroid or retina in any eye. (F) Collagen fibril bundles appeared regularly arranged, and magnified images (960× and 6800×) of a collagen fibril bundle of the sclera from all groups are shown above. The collagen fibrils in one bundle were oriented in the same direction. Scleral cells were localized between or within collagen fibril bundles. No abnormal changes were found in the treated eye compared with the untreated eye.

ability to control myopia progression with 4S-PEG scleral crosslinking.

3.3.3 Safety evaluation in rabbits. Retrobulbar injection, competently administered, is a safe and common procedure for ophthalmic therapy and surgery. As the pathological scleral changes in the progression of myopia are focused on the posterior pole of the eye, we improved the method of crosslinking by retrobulbar injections to facilitate the *in situ* crosslinking of the posterior sclera. However, there were safety issues requiring attention due to the proximity of the optic nerve and posterior retina. Kimball *et al.*[42] reported an increase in glaucoma damage in a mouse model when the entire sclera was crosslinked. Wang *et al.*[8] found apoptotic cells and ultrastructural changes in the retinal layers of eyes after scleral crosslinking. Therefore we investigated the possible pathological changes, including functional and structural changes, after retrobulbar injections of crosslinking agents by IOP, eye movement and by direct ophthalmoscopy and OCT. Furthermore, we evaluated the possible histological changes by H&E staining, TUNEL staining and transmission electron microscopy.

First, the fitting curve functions of the mean body weight between the two groups were almost coincident (Fig. 8A). There were no intergroup differences at any time point ($P > 0.05$, all), which implies that there was no difference between retrobulbar injection of 4S-PEG and PBS on the development of young rabbits.

As for IOP, the changes in the mean IOP were similar in the two groups. The mean IOP exhibited an increasing trend 7 days after the first injection in two groups but soon returned to baseline, which may be associated with the retrobulbar injection of high volumes of agents relative to the retrobulbar volume at an early age (Fig. 8B).

No restriction of eye movement was found in any group. The peripheral retina and optic nerve appeared normal in all eyes by direct ophthalmoscopy before the experiment and after every retrobulbar injection. OCT showed a normal retina and choroid after the injection of PBS or 4S-PEG (Fig. 8C). No signs of inflammation or abnormalities were observed in the treated eye compared with the unoperated left eye.

As shown in Fig. 8D, the retina, choroid, sclera and optic nerve in H&E-stained paraffin-embedded sections of the globe showed typical features. There was no evidence of pathological findings, such as necrosis, inflammation, degeneration or atrophy. The TUNEL assay, as a method for detecting apoptotic DNA fragmentation, has been widely used to identify and quantify apoptotic cells with high sensitivity and accuracy. Similar to the H&E staining results, no TUNEL and DAPI double-stained cells, *i.e.*, apoptotic cells, were observed in any of the layers of the globe (Fig. 8E). Transmission electron microscopy was conducted to evaluate changes in subcellular structures, especially collagen fibril/fibril bundle organization, in scleral tissue in the treated eye compared with the untreated eye. Collagen fibril bundles appeared regularly arranged, and collagen fibrils in one bundle were oriented in the same direction in electron micrographs of all layers of the sclera in all groups (Fig. 8F). It should be noted that the sclera from all treated eyes was observed to be normal. No histological differences were found between the untreated and treated eye specimens.

In summary, we found that all NHS-terminated PEG derivatives exhibited the expected relatively low cytotoxicity. Among them, 4S-PEG (MW = 10 000) showed the most significant improvement in the biophysical, biochemical and biological properties of the sclera. In rabbits, 4S-PEG (MW = 10 000) showed safe and effective control of the progression of form-deprivation myopia at a relatively low concentration (2.5 mM). The results of this work demonstrate that 4S-PEG can serve as a robust macromolecular crosslinking agent and is expected to have promise for application in the treatment of the progression of myopia.

4. Conclusions

In conclusion, 4S-PEG (MW = 10 000) are sufficiently safe for exposure to human fetal scleral fibroblasts and repeated retrobulbar injections in New Zealand rabbits over a period of 56 days. Treatment with 2.5 mM 4S-PEG (MW = 10 000) by retrobulbar injection effectively controlled the progression of form-deprivation myopia in rabbits and showed better efficacy in scleral crosslinking. Our study is an innovative trial of a branched PEG polymer utilized to prevent myopia progression. These findings will have important implications for fighting progressive myopia. Further investigations should address the long-term safety and biomechanical effects of crosslinking for the prevention of progressive myopia.

Author contributions

Yanbing Wang: conceptualization, methodology, software, investigation, visualization, formal analysis, data curation, writing-original draft preparation. Zhenquan Wu: methodology, investigation, validation. Jiang Lu: conceptualization. Silvia Tanumiharjo: editing. Jianbing Huang: conceptualization, writing-review & editing. Xiujuan Zhao: project administration, writing-review & editing. Lin Lu: conceptualization, project administration, supervision.

Conflicts of interest

There are no conflicts to declare.

Notes and references

1 B. A. Holden, T. R. Fricke, D. A. Wilson, M. Jong, K. S. Naidoo, P. Sankaridurg, T. Y. Wong, T. J. Naduvilath and S. Resnikoff, *Ophthalmology*, 2016, **123**, 1036–1042.
2 I. G. Morgan, K. Ohno-Matsui and S.-M. Saw, *Lancet*, 2012, **379**, 1739–1748.
3 A. E. Haarman, C. A. Enthoven, J. W. L. Tideman, M. S. Tedja, V. J. Verhoeven and C. C. Klaver, *Invest. Ophthalmol. Visual Sci.*, 2020, **61**, 49.
4 B. J. Curtin, T. Iwamoto and D. P. Renaldo, *Arch. Ophthalmol.*, 1979, **97**, 912–915.

5 N. A. McBrien and A. Gentle, *Prog. Retinal Eye Res.*, 2003, **22**, 307–338.
6 C. F. Wildsoet, A. Chia, P. Cho, J. A. Guggenheim, J. R. Polling, S. Read, P. Sankaridurg, S.-M. Saw, K. Trier and J. J. Walline, *Invest. Ophthalmol. Visual Sci.*, 2019, **60**, M106–M131.
7 G. Wollensak, E. Iomdina, D. D. Dittert, O. Salamatina and G. Stoltenburg, *Acta Ophthalmol. Scand.*, 2005, **83**, 477–482.
8 M. Wang, F. Zhang, K. Liu and X. Zhao, *Clin. Experiment Ophthalmol.*, 2015, **43**, 156–163.
9 E. Spoerl, M. Mrochen, D. Sliney, S. Trokel and T. Seiler, *Cornea*, 2007, **26**, 385–389.
10 A. Elsheikh, B. Geraghty, D. Alhasso, J. Knappett, M. Campanelli and P. Rama, *Exp. Eye Res.*, 2010, **90**, 624–633.
11 R. E. Norman, J. G. Flanagan, S. M. Rausch, I. A. Sigal, I. Tertinegg, A. Eilaghi, S. Portnoy, J. G. Sled and C. R. Ethier, *Exp. Eye Res.*, 2010, **90**, 277–284.
12 P. Mitchell, F. Hourihan, J. Sandbach and J. J. Wang, *Ophthalmology*, 1999, **106**, 2010–2015.
13 L. Xu, Y. Wang, S. Wang, Y. Wang and J. B. Jonas, *Ophthalmology*, 2007, **114**, 216–220.
14 G. Wollensak and E. Iomdina, *Acta Ophthalmol.*, 2008, **86**, 887–893.
15 Y. Chu, Z. Cheng, J. Liu, Y. Wang, H. Guo and Q. Han, *J. Ophthalmol.*, 2016, **2016**, 1–8.
16 A. Gautieri, F. S. Passini, U. Silván, M. Guizar-Sicairos, G. Carimati, P. Volpi, M. Moretti, H. Schoenhuber, A. Redaelli and M. Berli, *Matrix Biol.*, 2017, **59**, 95–108.
17 T. Girton, T. Oegema and R. T. Tranquillo, *J. Biomed. Mater. Res.*, 1999, **46**, 87–92.
18 T. X. Liu and Z. Wang, *Acta Ophthalmol.*, 2013, **91**, e253–e257.
19 T.-X. Liu and Z. Wang, *Int. J. Ophthalmol.*, 2017, **10**, 355.
20 M. Wang and C. C. C. Corpuz, *BMC Ophthalmol.*, 2015, **15**, 1–7.
21 M. El Hamdaoui, A. M. Levy, M. Gaonkar, T. J. Gawne, C. A. Girkin, B. C. Samuels and R. Grytz, *Transl. Vis. Sci. Technol.*, 2021, **10**, 1.
22 C. Wang, T. T. Lau, W. L. Loh, K. Su and D. A. Wang, *J. Biomed. Mater. Res., Part B*, 2011, **97**, 58–65.
23 A. Ozaki, M. Kitano, N. Furusawa, H. Yamaguchi, K. Kuroda and G. Endo, *Food Chem. Toxicol.*, 2002, **40**, 1603–1610.
24 M. Kim, A. Takaoka, Q. V. Hoang, S. L. Trokel and D. C. Paik, *Invest. Ophthalmol. Visual Sci.*, 2014, **55**, 3247–3257.
25 B. L. Banik and J. L. Brown, in *Natural and Synthetic Biomedical Polymers*, Elsevier, 2014, pp. 387–395.
26 G. T. Hermanson, *Bioconjugate techniques*, Academic press, 2013.
27 F. Keeley, J. Morin and S. Vesely, *Exp. Eye Res.*, 1984, **39**, 533–542.
28 G. Hermanson, *Bioconjugate techniques*, 2013, 3, pp. 229–258.
29 T. Taguchi, L. Xu, H. Kobayashi, A. Taniguchi, K. Kataoka and J. Tanaka, *Biomaterials*, 2005, **26**, 1247–1252.
30 M. Sanami, I. Sweeney, Z. Shtein, S. Meirovich, A. Sorushanova, A. M. Mullen, M. Miraftab, O. Shoseyov, C. O'Dowd and A. Pandit, *J. Biomed. Mater. Res., Part B*, 2016, **104**, 914–922.
31 K. E. Inostroza-Brito, E. C. Collin, A. Majkowska, S. Elsharkawy, A. Rice, E. Armando, X. Xiao, J. Rodríguez-Cabello and A. Mata, *Acta Biomater.*, 2017, **58**, 80–89.
32 G. Pasut and F. M. Veronese, *J. Controlled Release*, 2012, **161**, 461–472.
33 M. C. Parrott and J. M. DeSimone, *Nat. Chem.*, 2012, **4**, 13–14.
34 C. Weiyi, X. Wang, C. Wang, L. Tao, X. Li and Q. Zhang, *Clin. Biomech.*, 2008, **23**, S17–S20.
35 J. R. Phillips, M. Khalaj and N. A. McBrien, *Invest. Ophthalmol. Visual Sci.*, 2000, **41**, 2028–2034.
36 K. Chiu, L. L. Agoubi, I. Lee, M. T. Limpar, J. W. Lowe Jr and S. L. Goh, *Biomacromolecules*, 2010, **11**, 3688–3692.
37 N. A. McBrien, L. M. Cornell and A. Gentle, *Invest. Ophthalmol. Visual Sci.*, 2001, **42**, 2179–2187.
38 H. Xiao, Z.-Y. Fan, X.-D. Tian and Y.-C. Xu, *Int. J. Ophthalmol.*, 2014, **7**, 245.
39 D. Cui, K. Trier, J. Zeng, K. Wu, M. Yu, J. Hu, X. Chen and J. Ge, *Acta Ophthalmol.*, 2011, **89**, 328–334.
40 Z. Lin, X. Chen, J. Ge, D. Cui, J. Wu, F. Tang, J. Tan, X. Zhong and Q. Gao, *J. Ocul. Pharmacol. Ther.*, 2008, **24**, 543–550.
41 M. Funata and T. Tokoro, *Graefe's Arch. Clin. Exp. Ophthalmol.*, 1990, **228**, 174–179.
42 E. C. Kimball, C. Nguyen, M. R. Steinhart, T. D. Nguyen, M. E. Pease, E. N. Oglesby, B. C. Oveson and H. A. Quigley, *Exp. Eye Res.*, 2014, **128**, 129–140.